RESOURCE

Adjuvanted influenza-H1N1 vaccination reveals lymphoid signatures of age-dependent early responses and of clinical adverse events

Olga Sobolev[1–3,10], Elisa Binda[1,3,4,10], Sean O'Farrell[1–3], Anna Lorenc[3], Joel Pradines[5], Yongqing Huang[5], Jay Duffner[5], Reiner Schulz[3,6], John Cason[7], Maria Zambon[8], Michael H Malim[3,7], Mark Peakman[1,3], Andrew Cope[3,9], Ishan Capila[5], Ganesh V Kaundinya[5] & Adrian C Hayday[1–3]

Adjuvanted vaccines afford invaluable protection against disease, and the molecular and cellular changes they induce offer direct insight into human immunobiology. Here we show that within 24 h of receiving adjuvanted swine flu vaccine, healthy individuals made expansive, complex molecular and cellular responses that included overt lymphoid as well as myeloid contributions. Unexpectedly, this early response was subtly but significantly different in people older than ~35 years. Wide-ranging adverse clinical events can seriously confound vaccine adoption, but whether there are immunological correlates of these is unknown. Here we identify a molecular signature of adverse events that was commonly associated with an existing B cell phenotype. Thus immunophenotypic variation among healthy humans may be manifest in complex pathophysiological responses.

The profound impact of immunization on public health is well illustrated by the reported efficacy of an Ebola-specific vaccine[1,2]. Moreover, the potential applications of vaccines have broadened greatly as the biological implications of immunology have extended from infectious diseases, allergy and autoimmunity to metabolic disease[3], neurodegeneration[4] and cancer[5]. Yet because most immunological experiments are undertaken in mechanistically tractable model systems, the understanding of human immune response dynamics has lagged behind.

This situation has been somewhat redressed by 'systems vaccinology', faciliated advances in high-throughput analytical technologies and in informatics and biostatistics[6]. Thus, several studies have shown that many immunological metrics show little day-to-day variation[7,8], thereby permitting reliable measurements of responses to scheduled perturbations such as vaccination[6], immune checkpoint blockade[9] or iatrogenic immune suppression[10]. Nonetheless, more studies are required to help establish general principles—for example, whether there are consensus immune signatures predicting poor responsiveness to particular modalities and whether discrete immunological phenotypes might be linked to adverse events (AEs). Transient AEs (sometimes dismissed as 'man flu') can undermine herd immunity by provoking diminished vaccination compliance and even halting vaccine trials[11]. Additionally, there have been highly public concerns that vaccines may exacerbate preexisting pathologies.

Influenza virus causes serious, potentially life-threatening disease. Because of seasonal strain variation, annual vaccination is recommended[12]. However, owing to year-to-year similarity among seasonal flu strains, vaccine responses commonly reflect flu-specific memory cell reactivation[8,13]. Conversely, the human immune response dynamics (HIRD) study described here monitored the response to H1N1 'swine flu' that circulated in 2009 and was the first major H1N1 outbreak in several decades[14]. Whereas people older than 40 years might harbor swine flu–specific memory cells, this was unlikely in younger individuals who comprised the bulk of the HIRD cohort. Thus, the study offered an opportunity to investigate responses to flu vaccination that were not obviously dominated by recall responses.

Importantly, and in contrast to flu vaccines used in US immune-monitoring studies[8,13,15–17], the UK H1N1 Pandemrix vaccine used here includes an adjuvant, AS03, designed to enhance immunogenicity[18,19]. However, whether the early response differs quantitatively or qualitatively from nonadjuvanted flu vaccines has not hitherto been investigated by systems vaccinology. Interestingly, rather than being the sole province of myeloid cells, early phases of immune responses are increasingly acknowledged to include contributions from innate lymphoid cells and innate-like T cells, including γδ T cell cross-priming of CD8+ T cells[20–22]. Whether adjuvanted vaccines might promote such lymphoid stress surveillance is unknown.

The HIRD trial longitudinally tracked 178 healthy volunteers through two prevaccination and four post-vaccination time points. The trial's outcomes confirmed the practicality of high-throughput immune monitoring, which will be important as immunotherapies are more widely adopted. They established that within 24 h of receiving adjuvanted flu vaccine, healthy humans mount large and complex immune responses that include overt lymphoid contributions. This early response was slightly but substantially different in individuals aged more than ~35 years. In contrast to some reports[8,13,15–17], vaccine nonresponsiveness seemed to reflect broad human phenotypic variation rather than any consensus prevaccination immune signature. Conversely, post-vaccination AEs reported by ~20% of the study volunteers were associated with a discrete molecular signature that was in turn frequently associated with an atypical, prevaccination B cell phenotype. Thus, individual variation in immune composition can have complex pathophysiological manifestations. This notwithstanding, vaccination did not obviously exacerbate existing immune dysregulation.

RESULTS

Expansive transient responses to adjuvanted vaccination

From March 2010 to August 2011, the HIRD study enrolled 178 healthy adult volunteers (aged 18–65 years) with no known history of cancer, immunodeficiency, autoimmune or inflammatory diseases and no recent infection or vaccine exposure (**Table 1** and **Supplementary Table 1**).

Volunteers underwent a standard health examination, including blood and urine analysis, after which they completed six morning visits on prevaccination days −7 and 0 and post-vaccination days 1, 7, 14 and 63 (**Supplementary Fig. 1**). At each visit, fasting peripheral blood was sampled and banked. At the end of the day 0 visit, volunteers received a single intramuscular injection of the swine flu vaccine Pandemrix, which comprised 3.75 mg antigen from the A/California/7/2009 H1N1 virus strain in adjuvant AS03, which contains DL-α-tocopherol (vitamin E), squalene and polysorbate 80. At day 63, serological vaccine responses were measured at the UK Health Protection Agency (HPA) by both hemagglutination inhibition (HAI) and microneutralization (MN). Responders were defined, by convention, as those showing ≥4-fold increases in titer in one or both assays. Approximately 20% of volunteers were nonresponders (**Table 1**). At all visits, volunteers completed Likert wellness assessments[23], which showed that ~20% of males and ~25% of females experienced above-average clinical AEs, primarily at day 1 (**Table 1**). We assessed sera from 139 of the 178 volunteers by multiparameter Luminex and analyzed the white blood cells of 60 people from this subset by flow cytometry; from this group 46 individuals had their peripheral blood gene expression on days −7, 0, 1 and 7 assessed by microarray, (**Supplementary Fig. 1a**). Thus, all subjects whose gene expression was assessed were also assessed by all other methods. All platforms were subject to rigorous quality controls (Online Methods).

Of the volunteers analyzed, essentially all showed expansive changes in peripheral blood gene expression by day 1 (significant changes in ~9,000 gene probes ($P < 0.05$)) (**Supplementary Fig. 2a**), highly consistent with other studies that did not use adjuvants[8,16,24,25]. Quantitative reverse transcription PCR of 30 randomly selected genes across ~20 individuals provided independent validation of the microarray quantification at each time point (**Supplementary Fig. 2b,c**). Collective gene-expression patterns on day 1 differed significantly from those at prevaccination time points (days −7 and 0) as well as those on day 7 (**Fig. 1a**). Predictably, many of the genes most highly upregulated at day 1 encode and/or are associated with antigen presentation

Table 1 HIRD study overall cohort and subgroups of interest

Characteristic	HIRD study cohort	Serological vaccine nonresponders	Medium-high adverse events
	n	n	n
Total subjects (%)	178 (100)	35/166 (21.1)[a]	40/177 (22.6)[a]
Age			
Mean (s.d.)	28.7 (11.03)	29.1 (12.76)	27.6 (8.8)
Range	18.2–63.3	18.3–63.3	18.2–61.9
Sex			
Male (%)	70 (39.3)	14/66 (21.2)[b]	14/69 (20.3)[b]
Female (%)	108 (61.7)	21/100 (21.0)[b]	26/108 (24.1)[b]
Ethnicity			
Caucasian (%)	127 (71.4)	26 (74.3)	29 (72.5)
Asian (%)	24 (13.5)	6 (17.1)	5 (12.5)
Black/African (%)	10 (5.6)	2 (5.7)	2 (5.0)
Other (%)	17 (9.15)	1 (2.9)	4 (10.0)
Serological vaccine response			
HAI day −7, mean (s.d.)	56.05 (98.1)	155.2 (157.0)	72.0 (119.7)
HAI day 63, mean (s.d.)	451.5 (670.6)	265.1 (228.1)	461.5 (484.2)
HAI day 63/−7 ratio, mean (s.d.)	19.6 (43.8)	1.9 (0.9)	21.1 (32.0)
MN day −7, mean (s.d.)	361.4 (784.7)	1,194.0 (1,353.6)	524.3 (1,123.6)
MN day 63, mean (s.d.)	2,419.3 (2,008.4)	2,264.9 (1,941.6)	2,650.2 (2,072.1)
MN day 63/−7 ratio, mean (s.d.)	45.04 (85.23)	2.3 (0.9)	59.0 (112.8)
Adverse events combined day 1 and 7 score, mean (s.d.)	5.93 (4.76)	6.03 (5.30)	13.30 (3.74)

[a]Denominators <178 indicate exclusion of samples owing to test failure. [b]Percentage of males and females with the phenotype of total subjects of that sex in relevant cohort.

and interferon responses (**Fig. 1b**). Largely explaining this, most individuals at day 1 showed transient but significant (1.6-fold, on average) increases in the blood monocyte fraction and slight but significant decreases in numbers of recoverable peripheral blood cells (**Fig. 1c** and **Supplementary Fig. 2d**). Of note, for the 46 individuals assessed by microarray, the increases in monocyte numbers were significantly smaller than the changes (up to 160-fold) in expression of more than 135 genes, including those encoding activation-sensitive regulators (for example, *STAT1* (>16-fold) and *IRF1* (6-fold), *IRF7* (>3.5-fold), *IRF9* (>2.5-fold)), and markers of cell activation (for example, multiple genes encoding class II human leukocyte antigens (HLA-DR) (2- to 2.5-fold) and *TLR8* 3.5-fold) (**Supplementary Fig. 2e**). Thus, vaccination rapidly induced changes in peripheral blood mononuclear cell (PBMC) gene expression over and above the changes induced in PBMC composition. Most day 1 changes returned to baseline by day 7, by which time blood plasma cell counts were greatly increased, as was the expression of >1,000 genes, many associated with plasma cells (**Fig. 1a,b,d** and **Supplementary Fig. 2a**).

Changes in peripheral blood monocyte composition and gene expression at day 1 were associated with increased blood concentrations of cytokines and chemokines, notably CCL4, CCL2, interleukin 6 (IL-6) and granulocyte-colony stimulating factor (G-CSF), mostly attributable to myeloid cells[7,13,26] (**Fig. 1e**). Unexpectedly, however, the biggest fold-change was in interferon-γ (IFN-γ), a cytokine associated with type 1 helper T cells (T$_H$1 cells), cytolytic T cells, γδ T cells, natural killer T (NKT) cells, NK cells and type 1 innate lymphoid cells (**Fig. 1e**). Thus, the expansive, multifaceted transient changes in blood cell composition and gene expression that occurred within 24 h of receiving adjuvanted H1N1 vaccine included a distinct lymphoid contribution.

Figure 1 H1N1 vaccination leads to rapid and reversible early changes in the immune compartment, followed by a B cell–rich signature at day 7. (**a**) Observed values of multivariate statistic t (m.v.t.) quantifying global PBMC gene-expression dissimilarity in comparison of two study days (red dots) to values expected when days are randomly assigned between groups. Data show median and interquartile range; *$P < 0.0001$; **$P < 0.00005$; ***$P < 0.00001$; NS, not significant ($P > 0.05$). (**b**) Heat map of gene-expression levels of the 133 most altered genes ($\log_2$FC > 1; centered and scaled by gene across subjects and time points) on days −7, 0, 1 and 7; $n = 42$ (days −7 and 1), 43 (day 7) or 46 (day 0) subjects. (**c**) Average of fold changes (compared to prevaccination time points) per subject in PBMC immune cell subsets at days 1 and 7, determined by flow cytometry. $n = 46–65$ subjects; *$P < 0.05$, two-tailed paired t-test of % cell type at day 1 or 7, compared to both preimmune time points; †$P < 0.05$, only in comparison to day −7. (**d**) Average of fold changes (compared to prevaccination time points) per subject in B cell subsets at days 1 and 7, determined by flow cytometry. $n = 23–25$ subjects; P values as in **c**. (**e**) Average of fold changes (compared to prevaccination time points) per subject in serum cytokine and chemokine concentration at days 1 (blue) and 7 (red), determined by Luminex analysis.

$n = 96$ subjects for IL-13; 24 for IL-8, GM-CSF and CCL4; 123–134 for all other analytes. *$P < 0.05$, two-tailed paired t-test of serum analyte concentration at day 1, in blue, or 7, in red, compared to both preimmune time points, black.
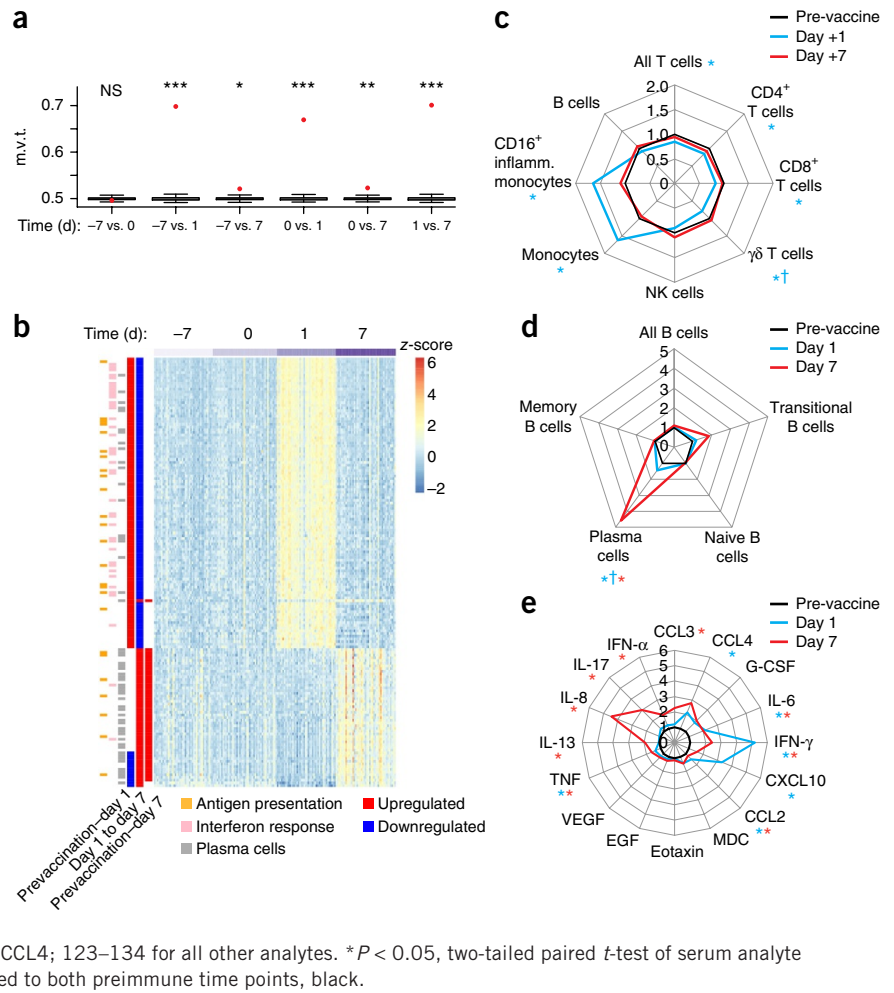
Early myeloid and lymphoid activation

The changes in day 1 peripheral blood monocyte composition and gene expression (**Supplementary Fig. 3a**) were reflected in monocyte activation, as evidenced by significant increases in the percentage of cells expressing HLA-DR and in the amount per cell of surface-expressed HLA-DR (**Fig. 2a,b**). By contrast, we observed significant, transient decreases in T cell representation and in transcripts encoding T cell functions, particularly signaling molecules (for example, *CD247*, *ZAP70*, *LCK*, *LAT* and *FYN*) (**Supplementary Fig. 3a** and **Fig. 2c**). These findings do not simply counter-balance the increases in blood monocytes, because the losses among CD8+ αβ T cells and γδ T cells were mostly confined to HLA-DR−CD38− cells. Thus, the blood became *de facto* enriched in activated lymphocytes, particularly HLA-DR+CD38+ cells (**Fig. 2d**).

A functional consequence of early myeloid and lymphoid activation was the overt upregulation of myriad interferon-stimulated gene transcripts (ISGs) (**Fig. 2e**). Although many ISGs probably reflected the actions of type I and III interferons (IFN-α and IFN-λ), they also included *CXCL9* (**Fig. 2e** and **Supplementary Fig. 2c**) which is much more strongly upregulated by IFN-γ. Moreover, the day 1 peak in blood protein concentration of CXCL10, which can be upregulated by IFN-α or IFN-γ, paralleled IFN-γ expression (**Fig. 2f**) rather than IFN-α expression, which peaked at day 7. Notably, the increases in IFN-γ and IFN-α serum protein concentrations were not mirrored in the transcripts of their encoding genes *IFNG* and *IFNA4* (or IFN-λ–encoding genes *IFNL1* and *IFNL2*) on day 1 or day 7 (**Fig. 2e**). This paradox might reflect enhanced interferon protein synthesis and/or

secretion rather than increased gene expression. Additionally, peripheral blood ISGs may have been upregulated by interferon proteins leaking into the blood from interferon-expressing cells within the vaccine injection site and/or the associated lymph nodes.

Among serum cytokines and chemokines, the most notable early marker of immune challenge was CXCL10, in part because baseline concentrations were consistently low: whereas >90% of 130 subjects had prevaccination CXCL10 concentrations <1 ng/ml, this was the median concentration by day 1 (**Fig. 2f**). Although significant ($P < 0.05$, two-tailed paired t-test) increases also occurred in tumor necrosis factor (TNF) and IL-6, the prevaccination concentrations of these cytokines showed high individual variation, which increased after vaccination (**Supplementary Fig. 3b**). Likewise, inter-individual variation largely obscured dynamic responses of other myeloid and lymphoid mediators, with post-vaccination expression of some molecules (such as IL-10) best described by a bimodal distribution (**Supplementary Fig. 3c**). This notwithstanding, significant ($P < 0.05$, two-tailed paired t-test) day 1 increases were evident for CCL5, another lymphoid cytokine (**Supplementary Fig. 3d**). In sum, adjuvanted H1N1 vaccine rapidly upregulated multiple myeloid and lymphoid effector functions, including type I and type II interferons.

Age affects early responses

This study was not designed to explore the well-established compromise in adaptive responses in subjects older than 70 (refs. 27,28). However, we unexpectedly identified subtle but significant impacts
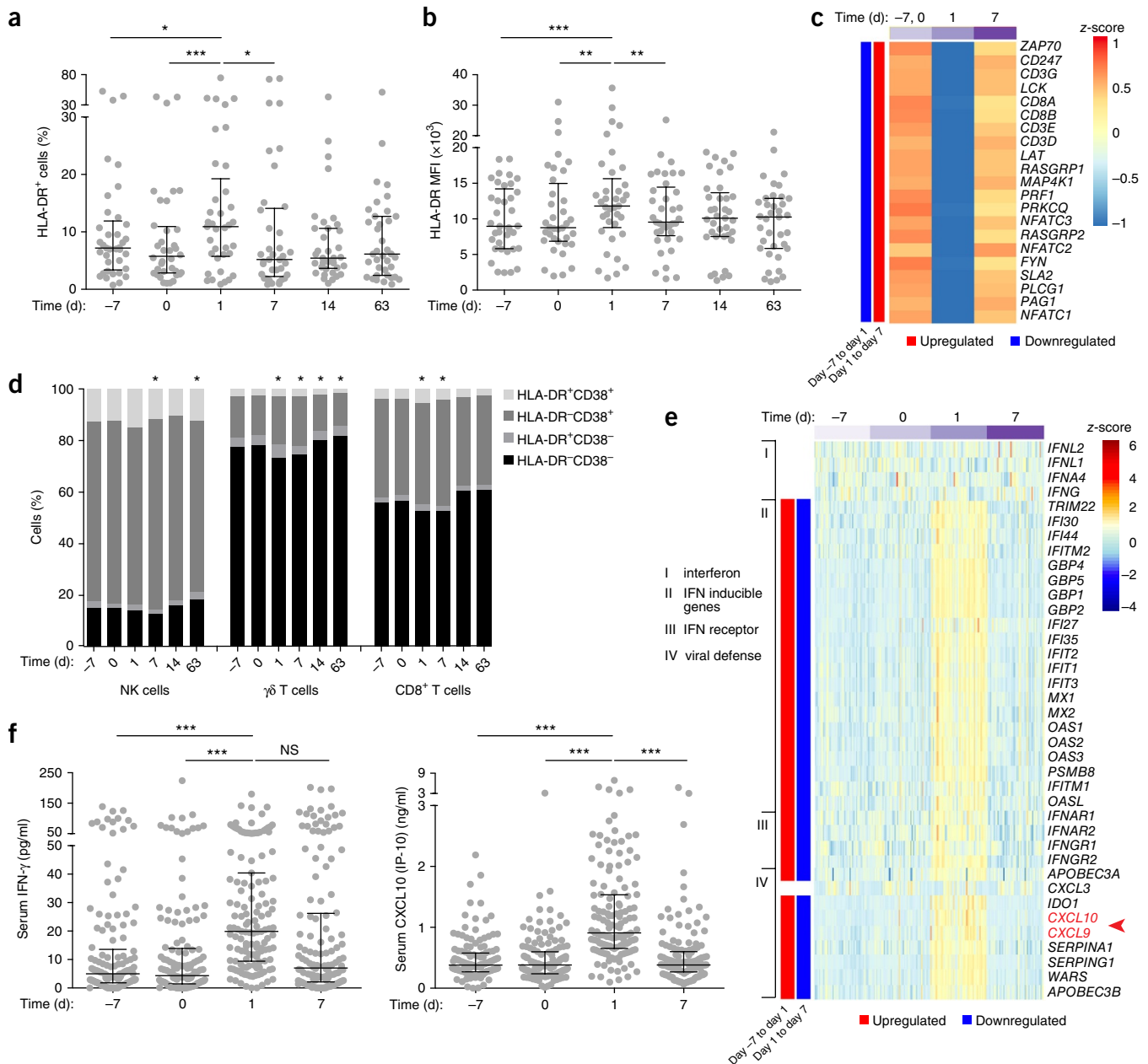
Figure 2 Early post-vaccine activation of myeloid and lymphoid cells is detectable across multiple assays. (**a,b**) Monocyte activation, assayed by flow cytometry of HLA-DR expression (**a**) and mean fluorescence intensity (MFI) (**b**) of live CD14+ cells. $n = 36–37$ subjects; points represent individual subjects; horizontal lines, median and interquartile range; *$P < 0.05$; **$P < 0.01$; ***$P < 0.00001$; NS, not significant ($P > 0.05$), two-tailed paired t-test. (**c**) Gene expression of T cell–specific genes (averaged across 46 subjects, centered and scaled by gene across time points). (**d**) Average percentage activation, assayed by flow cytometry, of HLA-DR and CD38 expression in CD8+ T cells, γδ T cells and NK cells ($n = 65$ subjects; *$P < 0.05$, two-tailed paired t-test of percentage of HLA-DR−CD38− cells, compared to both preimmune time points). (**e**) Expression of interferons and interferon-inducible genes before and after vaccination (centered and scaled by gene across all subjects and time points; arrowhead highlights *CXCL9* and *CXCL10* expression). (**f**) Luminex analysis of serum IFN-γ and CXCL10 (IP-10) concentrations ($n = 130–133$ subjects; points represent individual subjects; horizontal lines, median and interquartile range; ***$P < 0.00001$; NS, not significant ($P > 0.05$), two-tailed paired t-test.

of age on day 1 gene expression. Forty subjects for whom gene-expression data were available across two prevaccination and two postvaccination time points were grouped into successive younger and older subsets by a barrier method—that is, the youngest five were compared to the remaining 35 (i5); the youngest 6 to the remaining 34 (i6) and so on, through to the youngest 35 being compared to the remaining five (i35) (**Supplementary Fig. 4** and **Fig. 3a**). This revealed a pattern not seen when subjects were randomly partitioned into 10^5 different,

comparably sized groupings. Specifically, the aggregate day 1 gene-expression signature was significantly different when ranks above i19 (**Fig. 3b**) were compared with younger subjects. At this point of divergence in gene expression, the median ages of the comparison groups were >40 and ~22, respectively (**Fig. 3a**). Moreover, at i21, where divergence was very significant, the minimum age of the older group was ~30 (**Fig. 3a**). This indicated that significant changes in the early response profile may occur at 30–40 years

Figure 3 Age factor in multivariate analysis of gene expression based on all genes. (**a**) Age statistics for groups separated by barrier method (**Supplementary Fig. 4**) defining the maximum, median and minimum age of subjects assigned as 'young' and 'old' for each value of i in our subject cohort. (**b**) Increasing subject age rank plotted against permutation test P values for a multivariate statistic t (m.v.t.), which quantifies Pearson dissimilarity between age groups, representing all possible partitions of subjects into 2 age groups of at least 5 subjects. P values are estimated with respect to 10^5 random reassignments of age to subject. Vertical red line (**a**,**b**) indicates inflection point at which age factor becomes a significant influence (m.v.t. permutation $P < 0.05$) on gene expression in the day 1 data set.
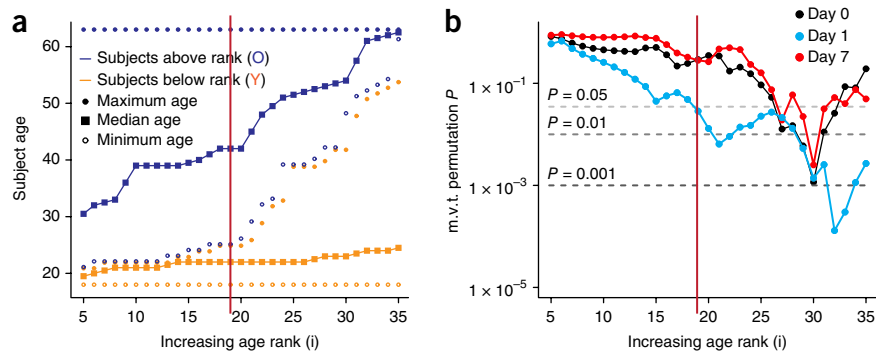
of age, much younger than is usually considered in the context of age-related immune dysregulation. Notably, transcripts underpinning the age-dependent differences included several that are functionally implicated in the early response (such as *TBX21*, *CD38* and *CD28*), and others implicated in immune regulation (such as *HDAC4*) (**Supplementary Table 2**).

Building on these findings we divided subjects into groups by age (above or below 35 years). The day 1 increases in IFN-γ and CXCL10 serum concentrations, and the peripheral blood lymphocyte (PBL) depletion of CXCR3+CD8+ T cells were all significantly lower in the older cohort ($P < 0.05$, IFN-γ and CXCL10 two-tailed Mann-Whitney test; CXCR, CD8 T cells two-tailed paired t-test) (**Supplementary Fig. 5a**,**b**). Although the most profound impact of age on gene expression was at day 1, there were also some significant differences in prevaccination lymphocyte subset counts in the older group (**Supplementary Fig. 5c**). Perhaps consistent with this, six age groupings (i27–i32) showed significant divergence in prevaccination gene expression (**Fig. 3b**).

It might be hypothesized that the difference in day 1 responses is a reflection of younger subjects' making primary responses versus older subjects' making efficacious recall responses. However, the changes in titer (0- to $>10^2$-fold) of influenza-specific antibodies, measured by HAI or MN, were spread similarly across subjects with low and high prevaccination titers and showed no correlation with age (**Supplementary Fig. 5d**). Consistent with this, the day 7 plasmablast-dominated gene-expression pattern was mostly unaffected by age (**Fig. 3b**), with only one group (i30) showing a substantial divergence, possibly reflecting its inclusion (relative to i31) of a profound nonresponder aged 48 years. In sum, the available data did not obviously support the idea that the early response in those aged more than ~35 years is altered by a shift toward making recall responses.

When we did an analogous assessment of subjects grouped by sex, the peripheral blood gene-expression patterns at all time points showed sexual dimorphism, as reported[29] (**Supplementary Fig. 5e**). However, this dimorphism was removed after normalization of gene expression at each time point to expression at day −7 prevaccination. Thus, the capacity of vaccination to induce expansive changes in gene expression was essentially unaffected by preexisting differences in the gene-expression profiles of males and females.

**Broad phenotypic variation underpins vaccine nonresponse**

Compliant with international guidelines, subjects showing ≥4-fold increases in influenza-specific antibodies measured by HAI and MN were defined as responders. Approximately 80% were responders (**Table 1** and **Fig. 4a**), whereas ~70% were reported as such in Pandemrix efficacy trials[18], probably reflecting HIRD's stringent exclusion criteria. We observed a complete spectrum of preexisting HAI and MN titers (**Fig. 4a**) among nonresponders, including 'baseline' nonresponders, whose low starting titers did not increase ≥4-fold, and 'glass ceiling' subjects, whose high starting titers made enhancements by ≥4-fold harder to achieve.

The frequency distribution of the day 63/day 7 MN titer ratios adhered to an additive model of two quasi-Gaussian distributions that respectively partitioned the HIRD cohort into one group with a very broad range of ratios between 0 and >30 and one with a narrow range of MN ratios, mostly ≤5 (**Fig. 4b**). This model suggests that nonresponders may have arisen from at least two groups of subjects, challenging the prospect of a consensus origin of vaccine failure. To further investigate this, we compared gene-expression patterns of 23 responders and 18 nonresponders. The most common nonresponse pattern was reduced expression of genes associated with plasma cell development and antibody production (**Fig. 4c**), as reported[8,17,24,30,31], coupled with a poor (albeit not absent) day 7 expansion of CD27+CD38hi plasmablasts (**Fig. 4d**). Conversely, B cell genes highly expressed by responders included three that were linked to responsiveness in other studies (*MZB1*, *TNFRSF17* and *XBP1*)[8,17,24,31] (**Supplementary Fig. 6a**).

Although nonresponders shared a failure to activate plasmablasts, there were many different 'routes to failure' as illustrated when we tracked the day −7, 0 (prevaccination), 1 and 7 gene-expression patterns, represented by principal components, for six baseline nonresponders relative to the consensus responder pattern (**Fig. 4e**). Thus, subject 402B did not significantly alter any genes; subject 39 altered many day 1 genes but returned to baseline; subject 3 started with an atypical pattern and regulated day 1 genes but did not progress beyond that; subject 11 regulated some genes on day 7 but without a preceding day 1 signature; subject 12 regulated day 1 genes but did not reach the day 7 signature; and subject 164 started with a highly atypical pattern and reverted toward the consensus prevaccination signature. Thus, nonresponders presented a broad spectrum of phenotypes.

Consistent with this, no common nonresponder signature could be found among individual and combinatorial cell phenotyping and analyte-expression patterns. There was a significant association with higher frequencies of activated γδ T and NK cells at all time points (**Supplementary Fig. 6b–d**), but these frequencies were so variable among individuals that high frequencies could not predict nonresponsiveness. Baseline nonresponders often showed higher IL-17 concentrations than responders and glass-ceiling nonresponders, but, again, IL-17 concentrations could not effectively segregate the groups (**Supplementary Fig. 6e**). In sum, neither molecular nor cellular data offered any consensus prevaccination predictor of nonresponsiveness akin to those proposed in studies of nonadjuvanted vaccines[8,16,17,24,31].
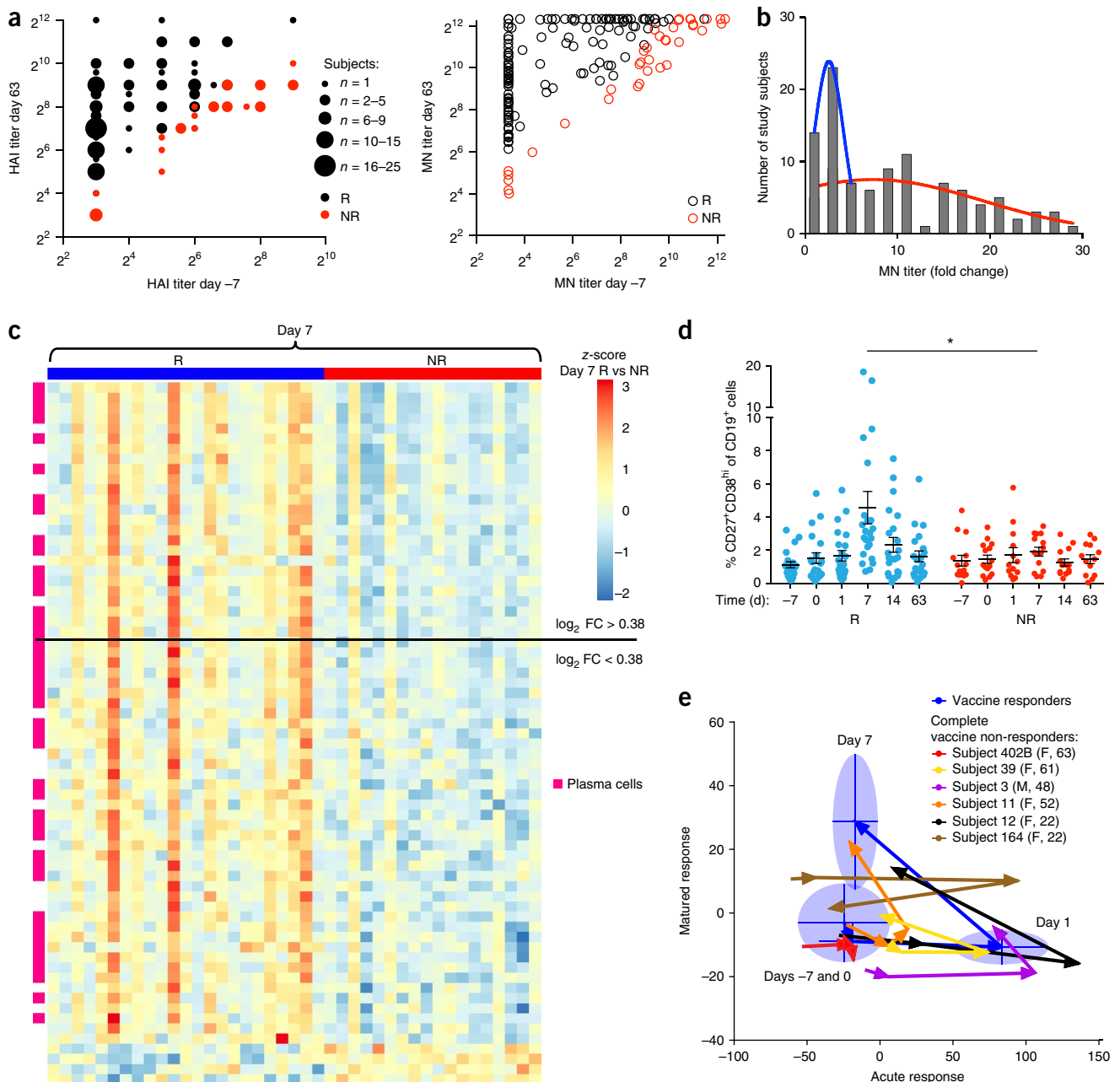
Figure 4 A vaccine nonresponse signature is detectable by post-vaccination day 7. (**a**) HAI and MN titers among HIRD study subjects at days −7 and 63. Data for subjects that did not show a four-fold increase in both titers (nonresponders (NR)) are shown in red; data for responders (R) in black. For HAI assay, marker sizes indicate the number of subjects with the same readout. (**b**) Fold change in MN titer (day 63 /day −7) described as a sum of two distributions, also identifying NR as a separate population (trendline fit $R = 0.8766$). Distribution 1 (blue), mean = 2.128 ± 0.581; distribution 2 (red), mean = 7.183 ± 12.30 (s.d.). (**c**) Genes expressed differentially between R ($n = 23$) and NR ($n = 18$) subjects at day 7 ($q < 0.05$, centered and scaled by gene across all subjects). (**d**) Flow cytometry analysis of plasma cell abundance in R and NR subjects at all time points (error bars, mean $\pm$ s.e.m. for $n = 20$–23 (R), 13–15 (NR); each point represents plasma cell percentage for an individual subject; *$P < 0.05$, two-tailed Mann-Whitney test). (**e**) Principal component analysis (PCA) of genes significantly altered at day 1 and day 7 ($P < 0.0001$ compared to combined prevaccination time points (day −7 and day 0)). PC1 from probes significantly altered at day 1 (acute response) is plotted against PC1 probes significantly altered at day 7 (matured response). Blue arrows indicate the average response for all vaccine responders at each time point; blue bars and ovals indicate area within ± 1 s.d. of vaccine responder average. Colored lines and arrowheads indicate trajectory of individual 'baseline' NR subjects, whose initial HAI and MN titers were at baseline prevaccination and did not increase. Subject sex (M, male; F, female) and age (y) at vaccination indicated in parentheses.

Peripheral blood signature of pathophysiology

Using well-established methods for quantifying patients' perception of symptoms such as pain[23], we assessed short-term clinical outcomes of all subjects across a spectrum of AEs (**Fig. 5a**). Most AEs were related to day 1, with fewer prolonged events captured from day 1 to day 7.

After pooling these two time points, we grouped subjects by high, medium and low AE. There was no obvious correlation between AEs and gender, age or vaccine responsiveness (**Table 1** and **Fig. 5b**).

Given that the HIRD cohort was healthy with no known immunological dysregulation, we initially considered that high and medium
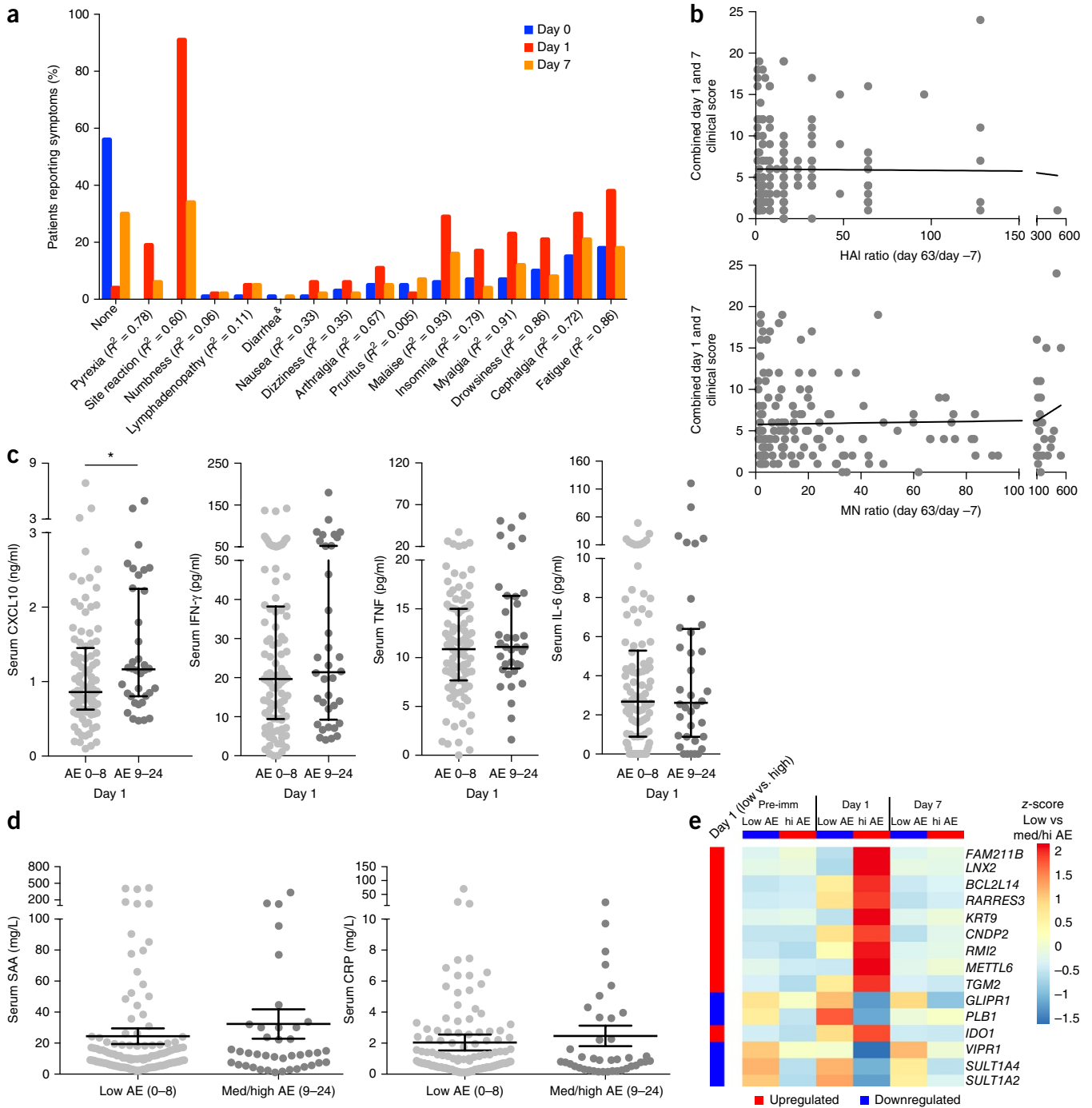
Figure 5 High AE individuals show day 1 and prevaccine differences from asymptomatic study subjects. (**a**) Distribution of symptoms before and after vaccination in the HIRD study cohort, expressed as percentage of subjects reporting a given symptom on study days 0, 1 and 14. R values in linear correlation of average day 1 and 7 score per subject for each symptom with the overall combined AE score are indicated; &, not reported on day 1. (**b**) Combined day 1 and 7 clinical score and HAI or NM day 63/day −7 titer ratio for the same individuals. $n = 176$ subjects, Pearson $r = 0.00022$ and 0.00723 for HAI and MN, respectively; $P > 0.05$ in both cases. (**c**) Luminex analysis of serum analyte concentrations at day 1 in low-AE versus medium-high (med/high)-AE subjects (each point represents an individual; horizontal lines, median and interquartile range; $n = 98$–100 (low AE) or 36–38 (med/high) AE subjects; *$P < 0.05$, two-tailed Mann-Whitney test. (**d**) Prevaccine serum amyloid A (SAA) and C-reactive protein (CRP) levels (average of days −7 and 0) in low AE ($n = 132$) and med/high AE ($n = 40$) study subjects. Data are mean ± s.e.m. (**e**) Gene-expression differences between low-AE (combined clinical score of 0–8) and med/high-AE (combined clinical score of 9–24) study subjects before and on days 1 and 7 after vaccination ($q < 0.05$, centered and scaled by gene across all subjects).

(high/medium) AEs might reflect exaggerated, innate-like recall responses of memory lymphocytes. However, neither prevaccination memory T cell numbers (**Supplementary Fig. 7a,b**) nor baseline

antibody titers were correlated with AEs. Although subjects with high/medium AEs collectively showed higher day 1 CXCL10 upregulation, inter-individual variation confounded the possibility of using
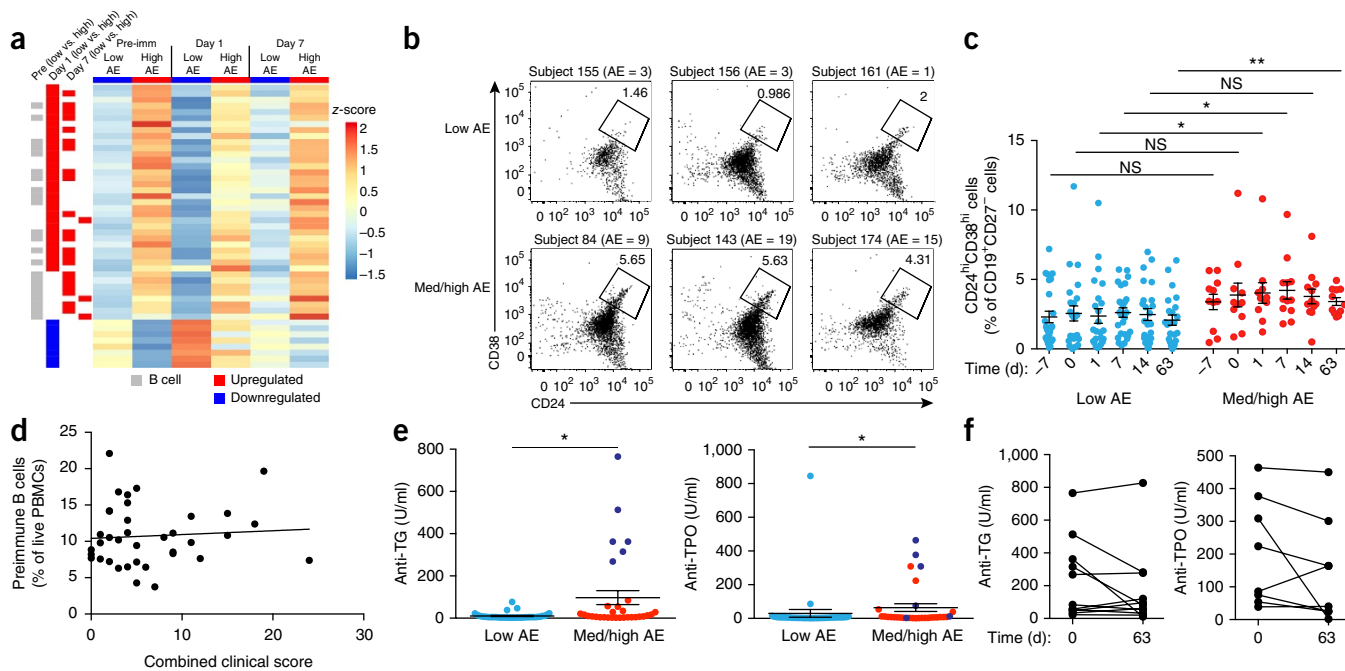
Figure 6 Prevaccine transitional B cell frequencies and increased autoantibodies correlate with post-vaccination AE. (**a**) Gene-expression differences between low-AE (clinical score 0–8) and medium-high (med/high)-AE (clinical score of 9–24) subjects prevaccination and on post-vaccine days 1 and 7 ($q < 0.05$, centered and scaled by gene across all subjects). (**b**) Flow cytometry plots of transitional B cell gating, showing percentages of transitional B cells (CD24hiCD38hi, indicated by outline and numbers) in live CD19+CD27– cells at day –7 in three low-AE and three med/high-AE subjects. (**c**) Flow cytometry analysis of transitional B cells at all study time points in low-AE and med/high-AE subjects ($n = 23$–26 and $n = 11$–12, respectively; each point represents transitional B cell percentage in an individual subject; error bars represent mean and s.e.m. for each time point; *$P < 0.05$; **$P < 0.01$; NS, not significant ($P > 0.05$), two-tailed Mann-Whitney test. (**d**) Prevaccination total B cell percentage (average of days –7 and 0 for each study subject, $n = 37$) versus combined day 1 and 7 AE score for the same individuals. Pearson r, $P > 0.05$. (**e**) Anti-thyroglobulin (anti-TG) and anti-thyroperoxidase (anti-TPO) serum antibody titers at day 0 in low-AE and med/high-AE subjects. Subjects with the 6 highest anti-thyroglobulin titers are indicated in purple. Error bars, mean ± s.e.m. within each subject group ($n = 37$ (low-AE) or 31 (med/high-AE) subjects); each point represents an individual subject. *$P < 0.05$, two-tailed Mann-Whitney test. (**f**) Anti-TG and anti-TPO titers at days 0 and 63; connected points represent measurements from the same subject. $n = 11$ (anti-TG) or 8 (anti-TPO) subjects.

CXCL10 concentrations to distinguish those with high/medium AEs (**Fig. 5c**). Moreover, AEs did not correlate with circulating TNF, IL-6 or IFN-γ concentrations or with commonly employed markers of inflammation, including serum amyloid A and C-reactive protein (**Fig. 5c,d**). By contrast, those with high/medium AEs showed notably higher transient day 1 expression of a small set of genes, including *LNX2*, *BCL2L14*, *RARRES3*, *KRT9*, *CNDP2*, *RM12* (*MRPL12*), *METTL6* and *TGM2* (**Fig. 5e**). Although it remains to be seen whether any such genes directly relate to clinical symptoms, their capacity to segregate the HIRD cohort into those with high/medium AEs asserts a bona fide peripheral blood signature of self-reported vaccination-associated illness.

Transitional B cells, autoimmunity and AEs

To investigate whether any prevaccination immunological profile might identify people prone to AEs, we further investigated differential gene expression. We found, unexpectedly, that the PBMCs of subjects with high/medium AEs overexpressed many B cell genes (relative to subjects with low AEs), before and after vaccination (**Fig. 6a** and **Supplementary Fig. 8a**). This signature often correlated with a prevaccination over-representation of CD27–CD38hiCD24hi transitional B cells (**Fig. 6b**), a trend that gained statistical significance immediately after vaccination (**Fig. 6c**). By contrast, AEs showed no association with total B cell counts (**Fig. 6d**).

Prevaccination transitional B cell numbers have been linked with nonresponsiveness after adjuvant-free flu vaccination[8]. However, our study found no correlation between vaccine efficacy and the percentages of transitional B cells, memory B cells or naïve B cells (**Supplementary Fig. 8b,c**), whether responsiveness was classified as a categorical variable (≥4-fold increases in titer) or as a continuous variable. Indeed, baseline nonresponders were spread across the full spectrum of transitional B cell subset representation (**Supplementary Fig. 8b**).

Interestingly, transitional B cell expansion has been associated with autoimmunity[32,33]. Therefore, to further test the unanticipated association of transitional B cells with pathophysiology, we investigated whether subjects with high/medium AEs might harbor autoantibodies despite being outwardly healthy. We found that 8 of 31 subjects with high/medium AEs, in contrast to only 1 of 37 subjects with low AEs, showed high-titer prevaccination reactivities to thyroglobulin and/or thyroid peroxidase, two specificities commonly tested for in the clinic (**Fig. 6e**). Of note, however, vaccination did not affect autoantibody titers, as assessed from day –7 to day 63 (**Fig. 6f**). In sum, there was within the healthy HIRD cohort a subpopulation with increased frequencies of transitional B cells, one-quarter of whom unknowingly harbored autoantibodies of potential clinical significance, and this subpopulation was more prone to developing AEs in response to adjuvanted H1N1 vaccine.

DISCUSSION

Vaccines remain a cardinal plank of public health, and several strategies are used to promote their immunogenicity. For example, an Ebola

vaccine reported in 2015 used vaccinia virus to deliver DNA encoding an Ebola antigen[2]. An alternative strategy delivers antigens in the context of adjuvants, such as AS03 in the Pandemrix H1N1 vaccine. AS03 markedly enhances B cell responses to bird flu when compared to another adjuvant, MF59, or to no adjuvant[34]. However, the human immune response to adjuvanted flu vaccines has not been assessed by systems vaccinology.

In that regard, our study shows that the Pandemrix H1N1 vaccine provokes rapid and expansive, yet transient, activation of myeloid cells and effectors, similarly to changes induced by other vaccines, including flu vaccines lacking adjuvant[8,13,15–17]. However, our study also reveals a pronounced lymphoid contribution to the early phase of the immune response, most evident in the prominent transient upregulation of IFN-γ, which was not apparent in most other virus vaccine studies. IFN-γ increases apparent at day 2 after administration of yellow fever vaccine[35] were not statistically significant. Conversely, IFN-γ RNA was upregulated in muscles of mice 4 h after injection of AS03 and viral antigens, with IFN-γ detected in the draining lymph nodes[19]. The functional consequences of IFN-γ upregulation remain to be clarified but may, at minimum, include CXCL9 and/or CXCL10 upregulation, as their expression closely paralleled that of IFN-γ in our study and in AS03-treated mice.

The issues remaining to be clarified include (i) the degree to which rapidly induced IFN-γ and/or other lymphoid effectors explain the efficacy of AS03 and other adjuvants, (ii) the cell types most responsible for the early lymphoid response and (iii) the molecular cues that promote the rapid activation of those cell types. For now, however, the data offer strong support for the idea that in some circumstances, lymphoid stress surveillance may be a key component to the early phase of the immune response. In that regard, the early enrichment for HLA-DR^{+}CD38^{+} activated effector T cells in our study contrasted with delayed increases in those cells after smallpox or yellow fever vaccination[35,36].

Within the HIRD cohort, a prominent day 7 plasmablast signature correlated strongly with vaccine responsiveness, as was true for several flu and other viral vaccines. Nonetheless, the size of the HIRD study exposed the large scale of human immunophenotypic variation and, therein, the many routes by which plasmablast activation may fail. Thus, the HIRD study did not identify a consensus prevaccination predictor of nonresponsiveness. This was true even when the convention of using ≥4-fold increases to define responders was substituted with a continuous range and when markers and predictors of nonresponsiveness reported by others[8,13,15–17] were specifically investigated (although we did not perform a detailed examination of follicular helper T cells[8,37]. There was also no association of HLA haplotype with any criteria measured in the HIRD study.

The difficulty in identifying a consensus nonresponder signature seems consistent with a published twin study that suggests that phenotypic, experiential variation has a more profound effect on vaccine responses than genetics[38]. Wide-ranging immunophenotypic variation may likewise underlie current difficulties in identifying predictive signatures of nonresponsiveness in cancer immunotherapy. Conversely, the emergence in HIRD and other trials of markers, particularly CXCL10 (ref. 24), that robustly reflect recent immunological challenge may form the basis of a consensus 'immune responsiveness signature' by which patient responses to a spectrum of interventions can be easily gauged in the clinic.

Age is a fundamental component of experiential variation, and marked declines in adaptive responsiveness in the elderly are well known and increasingly well understood[7,27,39,40]. By contrast, age-related differences in the early (day 1) response, such as those described here, have not been widely considered. Moreover, those

differences appeared to emerge at younger ages (~35 years) than are usually considered in the context of age-related immune dysregulation. Neither the basis nor consequences of those differences are yet known, but the findings emphasize how responses to vaccines, allergens and infections might be different for younger adults, with the potential to influence the design of efficacious vaccines and immune-therapeutics.

Whereas there may be many ways to fail to make an effective vaccine response, there may be only few routes to developing AEs of the broad spectrum assessed in this study. Vaccine-related AEs can pose serious obstacles to vaccine approval and to public compliance with vaccination regimens. Thus, concrete cellular and molecular patterns associated with symptoms of AEs may offer ways to limit such events and/or stratify patients. In this regard, our study provides evidence that high/medium AEs reported equally by men and women are associated with a discrete post-vaccination gene signature. Most unexpectedly, however, AEs were also associated with a prevaccination gene-expression pattern that was in turn commonly manifest in an atypical B cell phenotype. Moreover, this atypical phenotype predicted that several subjects reporting AEs harbored autoantibodies. More than one-quarter of the medium/high-AE cohort scored positive in tests of only two clinically relevant specificities. Thus, whereas it is well established that human immonophenotypic variation can affect immune responses to pathogens and/or provoke clinical autoimmunity, our study has established how such variation in healthy adults may also be associated with complex, subclinical pathophysiology whose consequences are manifest only on challenge and whose read-outs are not overtly immunological. Therefore, as algorithms and data-analysis tools grow in power, together with clinical phenotyping and molecular pathology, so practical monitoring of peripheral blood may identify discrete forms of human immunophenotypic variation that collectively predict a broad spectrum of pathophysiological conditions and/or responses to treatment.

METHODS
Methods and any associated references are available in the online version of the paper.

AUTHOR CONTRIBUTIONS
O.S. and E.B. coordinated experiments, designed and undertook phenotypic analyses of PBMC and sera and contributed to data analysis; S.O'F. designed and undertook molecular analyses of PBMC gene expression and provided data analyses; A.L., J.P., Y.H., J.D. and R.S. developed and applied statistical and bioinformatics tools for data analysis and presentation; J.C. supervised and undertook PBMC sample preparation and biobanking; M.Z. supervised and undertook HAI and MN assays of antibody titers; M.H.M. helped devise the study, oversaw biobanking and edited the manuscript; M.P. and A.C. oversaw

and implemented T cell assays, clinical assessment measures and obtainment of ethical approval; I.C. and G.V.K. devised and implemented integrative data analysis strategies, prepared figures and edited the manuscript. A.C.H. designed and supervised the study, cowrote documents for ethical approval, reviewed all data sets and wrote and edited the manuscript with O.S. and S.O'F.

COMPETING FINANCIAL INTERESTS

The authors declare no competing financial interests.

Reprints and permissions information is available online at http://www.nature.com/reprints/index.html.

1. Agnandji, S.T. *et al.* Phase 1 trials of rVSV Ebola vaccine in Africa and Europe—preliminary report. *N. Engl. J. Med.* doi:10.1056/NEJMoa1502924 (1 April 2015).
2. Henao-Restrepo, A.M. *et al.* Efficacy and effectiveness of an rVSV-vectored vaccine expressing Ebola surface glycoprotein: interim results from the Guinea ring vaccination cluster-randomised trial. *Lancet* **386**, 857–866 (2015).
3. Gregor, M.F. & Hotamisligil, G.S. Inflammatory mechanisms in obesity. *Annu. Rev. Immunol.* **29**, 415–445 (2011).
4. Czirr, E. & Wyss-Coray, T. The immunology of neurodegeneration. *J. Clin. Invest.* **122**, 1156–1163 (2012).
5. Chen, D.S. & Mellman, I. Oncology meets immunology: the cancer-immunity cycle. *Immunity* **39**, 1–10 (2013).
6. Pulendran, B. Systems vaccinology: probing humanity's diverse immune systems with vaccines. *Proc. Natl. Acad. Sci. USA* **111**, 12300–12306 (2014).
7. Duffy, D. *et al.* Functional analysis via standardized whole-blood stimulation systems defines the boundaries of a healthy immune response to complex stimuli. *Immunity* **40**, 436–450 (2014).
8. Tsang, J.S. *et al.* Global analyses of human immune variation reveal baseline predictors of postvaccination responses. *Cell* **157**, 499–513 (2014).
9. Callahan, M.K., Wolchok, J.D. & Allison, J.P. Anti-CTLA-4 antibody therapy: immune monitoring during clinical development of a novel immunotherapy. *Semin. Oncol.* **37**, 473–484 (2010).
10. Oswald, M. *et al.* Modular analysis of peripheral blood gene expression in rheumatoid arthritis captures reproducible gene expression changes in tumor necrosis factor responders. *Arthritis Rheumatol.* **67**, 344–351 (2015).
11. Chen, R.T. *et al.* The Vaccine Adverse Event Reporting System (VAERS). *Vaccine* **12**, 542–550 (1994).
12. Grohskopf, L.A. *et al.* Prevention and control of seasonal influenza with vaccines: recommendations of the Advisory Committee on Immunization Practices (ACIP)–United States, 2014–15 influenza season. *MMWR* **63**, 691–697 (2014).
13. Furman, D. *et al.* Apoptosis and other immune biomarkers predict influenza vaccine responsiveness. *Mol. Syst. Biol.* **9**, 659 (2013).
14. Zimmer, S.M. & Burke, D.S. Historical perspective—emergence of influenza A (H1N1) viruses. *N. Engl. J. Med.* **361**, 279–285 (2009).
15. Nakaya, H.I. *et al.* Systems biology of vaccination for seasonal influenza in humans. *Nat. Immunol.* **12**, 786–795 (2011).
16. Bucasas, K.L. *et al.* Early patterns of gene expression correlate with the humoral immune response to influenza vaccination in humans. *J. Infect. Dis.* **203**, 921–929 (2011).
17. Li, S. *et al.* Molecular signatures of antibody responses derived from a systems biology study of five human vaccines. *Nat. Immunol.* **15**, 195–204 (2014).
18. Roman, F. *et al.* Effect on cellular and humoral immune responses of the AS03 adjuvant system in an A/H1N1/2009 influenza virus vaccine administered to adults during two randomized controlled trials. *Clin. Vaccine Immunol.* **18**, 835–843 (2011).
19. Morel, S. *et al.* Adjuvant system AS03 containing α-tocopherol modulates innate immune response and leads to improved adaptive immunity. *Vaccine* **29**, 2461–2473 (2011).
20. Strid, J., Sobolev, O., Zafirova, B., Polic, B. & Hayday, A. The intraepithelial T cell response to NKG2D-ligands links lymphoid stress surveillance to atopy. *Science* **334**, 1293–1297 (2011).
21. Wencker, M. *et al.* Innate-like T cells straddle innate and adaptive immunity by altering antigen-receptor responsiveness. *Nat. Immunol.* **15**, 80–87 (2014).
22. Brandes, M. *et al.* Cross-presenting human γδ T cells induce robust CD8+ αβ T cell responses. *Proc. Natl. Acad. Sci. USA* **106**, 2307–2312 (2009).
23. Bolognese, J.A., Schnitzer, T.J. & Ehrich, E.W. Response relationship of VAS and Likert scales in osteoarthritis efficacy measurement. *Osteoarthritis Cartilage* **11**, 499–507 (2003).
24. Obermoser, G. *et al.* Systems scale interactive exploration reveals quantitative and qualitative differences in response to influenza and pneumococcal vaccines. *Immunity* **38**, 831–844 (2013).
25. Franco, L.M. *et al.* Integrative genomic analysis of the human immune response to influenza vaccination. *eLife* **2**, e00299 (2013).
26. Querec, T. *et al.* Yellow fever vaccine YF-17D activates multiple dendritic cell subsets via TLR2, 7, 8, and 9 to stimulate polyvalent immunity. *J. Exp. Med.* **203**, 413–424 (2006).
27. Montecino-Rodriguez, E., Berent-Maoz, B. & Dorshkind, K. Causes, consequences, and reversal of immune system aging. *J. Clin. Invest.* **123**, 958–965 (2013).
28. Jiang, N. *et al.* Lineage structure of the human antibody repertoire in response to influenza vaccination. *Sci. Transl. Med.* **5**, 171ra19 (2013).
29. Whitney, A.R. *et al.* Individuality and variation in gene expression patterns in human blood. *Proc. Natl. Acad. Sci. USA* **100**, 1896–1901 (2003).
30. Nakaya, H.I. *et al.* Systems biology of vaccination for seasonal influenza in humans. *Nat. Immunol.* **12**, 786–795 (2011).
31. Querec, T.D. *et al.* Systems biology approach predicts immunogenicity of the yellow fever vaccine in humans. *Nat. Immunol.* **10**, 116–125 (2008).
32. Yang, M., Rui, K., Wang, S. & Lu, L. Regulatory B cells in autoimmune diseases. *Cell. Mol. Immunol.* **10**, 122–132 (2013).
33. Engel, P., Gómez-Puerta, J.A., Ramos-Casals, M., Lozano, F. & Bosch, X. Therapeutic targeting of B cells for rheumatic autoimmune diseases. *Pharmacol. Rev.* **63**, 127–156 (2011).
34. Jackson, L.A. *et al.* Effect of varying doses of a monovalent H7N9 influenza vaccine with and without AS03 and MF59 adjuvants on immune response: a randomized clinical trial. *JAMA* **314**, 237–246 (2015).
35. Neves, P.C.da C., Matos, D.C.de S., Marcovistz, R. & Galler, R. TLR expression and NK cell activation after human yellow fever vaccination. *Vaccine* **27**, 5543–5549 (2009).
36. Miller, J.D. *et al.* Human effector and memory CD8+ T cell responses to smallpox and yellow fever vaccines. *Immunity* **28**, 710–722 (2008).
37. Bentebibel, S.-E. *et al.* Induction of ICOS+CXCR3+CXCR5+ T$_H$ cells correlates with antibody responses to influenza vaccination. *Sci. Transl. Med.* **5**, 176ra32 (2013).
38. Brodin, P. *et al.* Variation in the human immune system is largely driven by non-heritable influences. *Cell* **160**, 37–47 (2015).
39. Shin, M.S. *et al.* Maintenance of CMV-specific CD8+ T cell responses and the relationship of IL-27 to IFN-γ levels with aging. *Cytokine* **61**, 485–490 (2013).
40. Fülöp, T., Larbi, A. & Pawelec, G. Human T cell aging and the impact of persistent viral infections. *Front. Immunol.* **4**, 271 (2013).

ONLINE METHODS

Study design. From March 2010 to August 2011, 178 healthy adult volunteers (18–65 years of age) with no known history of cancer, autoimmune or inflammatory diseases were recruited for an experimental, before-and-after observational cohort study of Human Immune Response Dynamics (HIRD) after vaccination (**Table 1**). Each volunteer completed 6 visits: two prevaccination, at days −7 and 0, and four post-vaccination, at days 1, 7, 14 and 63.

At day −7, the subjects filled out a personal and family history health questionnaire and underwent a standard health examination, including full blood and urine analysis. Study exclusion criteria (**Supplementary Table 1**) were largely applied at this point. At the end of the day 0 visit, participants received a single intramuscular injection, administered according to the manufacturer's instructions, of the GlaxoSmithKline (GSK) Pandemrix H1N1 swine flu vaccine (comprising 3.75 mg antigen derived from A/California/7/2009 H1N1 virus strain and GSK proprietary adjuvant system AS03 containing DL-α-tocopherol, squalene and polysorbate 80). Study participants donated 2 baseline blood samples on days −7 and 0 before H1N1 vaccination (total blood volume 150 ml), followed by further donations on days 1, 7, 14 (each 60 ml) and day 63 (150 ml), totaling 540 ml (similar to a standard blood donation volume). Blood was drawn between 7:30 a.m. and 10:30 a.m. after fasting from midnight. At each visit, subjects completed a self-reported wellness assessment on the Likert scale to monitor for adverse events (AEs).

The study was reviewed by the Executive Board of the Biomedical Research Centre (BRC) of Guy's and St Thomas' Hospitals and King's College London, and approved by the Research Ethics Committee (REC study number 09/H0717/88). All volunteers gave informed consent to take part. The conditions of ethical approval required the study be completed for all volunteers after the day 63 visit and that we informed affected individuals of any deleterious metrics uncovered.

Sample processing and storage. Blood samples were drawn in the Clinical Research Facility of St Thomas' Hospital, transported to the main investigators' laboratories at King's College London, where immune cells, serum and plasma were purified by standard procedures. Cells, serum, DNA and plasma were preserved according to standard protocols dictated by downstream studies (for example, cryopreservation of 'live cells' for functional analyses; snap-freezing of cells in RNA preservative for analysis of gene expression). Samples were stored in the King's College London BRC BioBank facility. Cryopreserved cells were held in liquid nitrogen until required; all other samples were stored at −80 °C.

Defining serological vaccine response. Immune response to vaccine was assessed by H1N1-specific hemagglutination (HAI) and microneutralization (MN) assays carried out by the Health Protection Agency, UK, according to standard protocols. Assays were conducted on samples collected on day −7 and day 63, and day 63/−7 HAI and MN ratios determined. A vaccine responder was defined as an individual whose HAI and MN ratios were both ≥4.

Defining adverse events. For the 16-parameter wellness assessment, participants self-reported the intensity of each parameter on the Likert scale of 0–3. Parameters assessed were: site reaction to vaccine, fever, headache, tiredness, muscle ache, joint ache, swollen glands, numbness, sleepiness, dizziness, diarrhea, nausea, itching, sleeplessness, general unwellness, and any required use of painkiller. The AE score was calculated for each participant as a sum of all individual scores on every parameter on day 1 and from day 1 to day 7. The AE range for the HIRD study was 0–24, with a mean of 5.9 ± 4.8 (s.d.) and a median of 5 (Q1–Q3, 2–8). For the purposes of our study, scores of 0–8 were defined as low AE, scores above the third quartile, 8–16, were defined as medium AE, and scores above 16 (more than 2 s.d. above the mean) were defined as high AE. Of note, even the high-AE scores reflect an acute overt event of insufficient magnitude to merit medical consultation.

Experimental procedures and quality control. Immune phenotypes were assessed by Flow Cytometry in the Department of Immunobiology and in the BRC core facility, according to standard operating procedures (SOPs). In brief:

1. Multi-parameter polychromatic flow cytometry was performed on PBMC samples of 60 study participants to define white blood cell subset composition, activation state, and function. To achieve this, cryopreserved cells were thawed, washed and rested for 1 h, before Fc blocking with KIOVIG (human normal immunoglobulin, Baxter) followed by staining with relevant monoclonal antibodies (full staining panels described in **Supplementary Table 3**) and acquisition on the BD LSRFortessa analyzer, which was precisely calibrated to the same run parameters for each day of sample acquisition. Data were analyzed using FlowJo software. To control for day-to-day variation, PBMC samples from two individuals were prepared in a way identical to the study samples, and stored as large batches. These two individual samples were included in each experiment and used as an internal longitudinal standard in all flow cytometry assays. Antibody manufacturers and clone numbers are listed in **Supplementary Table 3**.

2. Multiplex serum cytokine analysis was performed on cryopreserved serum aliquots using the Luminex Flexmap 3D analyzer and the 39-plex and 16-plex human cytokine kits (Merck Millipore), according to the manufacturer's instructions. Each analysis included its own standard curve for every analyte; in addition, to control for any day-to-day experimental variation, two longitudinal control serum samples were included in each run.

3. Serum amyloid A (SAA); C-reactive protein (CRP), and autoantibody assays (antinuclear antibodies, ANA, using the Hep2 reporter cell assay; anti-rheumatoid factor, RF, using latex-enhanced turbidimetry; and anti-thyroglobulin, TH, and anti-thyroid peroxidase, TPO, ELISA assays) were carried out according to standard clinical testing protocols at the Immunology Diagnostic Laboratory, King's College Hospital, London.

4. HLA haplotype analysis for HLA-A*01, HLA-A*02, HLA-A*03, HLA-A*11, HLA-B*07, HLA-B*27, HLA-DRB1 and HLA-DRB3/4/5* was carried out by the Clinical Transplantation Laboratory at Guy's Hospital, London, according to standard protocols, on DNA obtained from frozen granulocyte samples.

Microarray analysis. Samples from days −7, 0, 1 and 7 for 46 of the study participants were selected without bias for microarray analysis. The samples were chosen from subjects representative of our overall cohort, and included vaccine responders (R, 34/46) and nonresponders (NR, 12/46; 6/46 baseline nonresponders, with no detectable preexisting H1N1 antibody response and no increase in post-vaccine antibody titers by either HAI or MN) and low (32/46) and medium/high (14/46) AE subjects.

RNAs extracted from PBMCs were processed in two batches according to the Agilent protocol and with Agilent Gene Expression Hybridization Kit, then hybridized to Agilent 4x44K v2 Human Whole Genome microarrays and scanned using Agilent's Microarray Scanner System (Agilent Technologies).

After QC, 173 arrays were retained in the analysis and the batch effect was removed with the method ComBat from the R package sva version 3.6.0 (http://www.bioconductor.org/). Further preprocessing (quantile normalization and subtraction of background estimated with method normexp) was completed with R package Agi4x44PreProcess (https://bioc.ism.ac.jp/packages/2.12/bioc/html/Agi4x44PreProcess.html). Only probes passing default good quality features filter from Agi4x44 were retained, resulting in 27,879 probes.

Initial analysis of the microarray gene-expression data was performed at the level of entire samples to assess data quality and detect potential differences between groups of samples (for example, males versus females). To perform such analysis, each sample i is represented by the vector x_i of $\log_2$ intensity values over all probes. Overall dissimilarity between two samples i and j is quantified with $d_{ij} = (1 - c(x_i, x_j))/2$, where c stands for the Pearson correlation coefficient. Perfect similarity between two samples corresponds to $d_{ij} = 0$ and perfect dissimilarity to $d_{ij} = 1$. Dissimilarities can be used for instance to perform hierarchical clustering of samples.

More quantitative statements regarding separation between two groups G and H of samples are obtained as follows. First, the following multivariate statistic t (m.v.t.) is estimated: $t(G, H) = d(G, H)/(s(G) + s(H))$ with

$$d(G,H) = \frac{1}{|G||H|}\Sigma_{i \in G, j \in H} d_{ij} \, , \; s(G) = \frac{2}{|G|(|G|-1)}\Sigma_{i < j \in G} d_{ij}$$

and where $|G|$ stands for the size of group G. Just like the univariate t-statistic, m.v.t. takes into account both difference between groups and spread within each group. Next, observed values of $t(G, H)$ were compared to values $T(G, H)$ expected when randomly reassigning samples between the two

groups. Namely, 10^5 realizations of the Fisher-Yates shuffle are used to estimate $p = Pr(T \geq t)$. An important advantage of such a permutation test is that it takes into account correlation between probes.

Analysis of potential effect on gene expression of subject age presented additional challenges and was conducted as follows. Because factor day has a strong effect on gene-expression patterns, effect of age is investigated at each day separately. To enable comparison of age effect at different days, the data set is reduced to the 40 subjects having gene-expression data for days 0, 1 and 7. Using m.v.t. to examine age effect requires defining age groups for permutation testing. An exhaustive approach to defining age groups consists in enumerating all possible partitions of subjects into 'young' (Y) and 'old' (O) groups of size at least 5 and reporting m.v.t. P values for each partition. Such enumeration is performed via a "barrier" approach: subjects are sorted by ascending age and the first r (Y) are compared to the remaining $40 - r$ (O). The profile of m.v.t. P values as a function of age rank r ($5 \leq r \leq 35$) provides an estimate of effect of subject age on gene expression. When subjects have the same age on both immediate sides of the barrier, all possible partitions are enumerated and the reported m.v.t. P value is the average over these partitions.

To find specific genes changing expression levels upon vaccination, we used all QC-approved samples and fitted (with R package limma) a linear model with time point as categorical variable, treating both time points before vaccination as repeated measures and subject as a blocking variable. Genes with expression levels different between any two time points (before vaccination, 1 d after, 7 d after) were identified by moderated t-test; cut-offs for q value and fold change were 0.05 and 1.5 or 2. For genes with several probes per gene, per-probe information was collapsed to per-gene information by arbitrary picking a probe with lower P value in first day after vaccination to prevaccination comparison in all individuals.

To find genes expressed differentially in vaccine responders and nonresponders, only individuals with samples available from both post-vaccination and a prevaccination time points were analyzed (39 individuals). Three different approaches were used. To detect genes expressed differently between Rs and NRs at separate time points, a linear model was fitted with limma, with responder status and time point as categorical variables and individual treated as a blocking variable. To detect genes with change in expression between time points different between Rs and NRs, prevaccination expression level was treated as a baseline and subtracted from later measurements; then genes changing differently were identified with limma-fitted linear model (time and responder status as categorical variables) and moderated t-test, or by fitting time course quadratic profiles with maSigPro (https://bioc.ism.ac.jp/packages/2.12/bioc/html/maSigPro.html). Unless otherwise mentioned, cut-offs for q value and fold change were 0.05 and 0.5.

Differences between individuals with and without AEs were identified in the same way as described for differences between responders and nonresponders, with low and medium/high AE defined as above.

Statistical analysis. Statistical analysis, significance cut-offs, and other analyses for the microarray data were performed following standard array analysis techniques. Flow cytometry, serum biochemistry, and serum analyte data were analyzed using Prism software. Data are reported as mean ± s.d. or median and interquartile range. Multiple samples were compared using one-way ANOVA where all data points for each sample were available, and using the Wilcoxon rank sum test, Student's t-test, or the Mann-Whitney nonparametric test, as appropriate to the analysis. Categorical data were compared by calculating the standard Normal deviate and two-tailed P value and are reported as mean (95% confidence interval).

Corrigendum: Adjuvanted influenza-H1N1 vaccination reveals lymphoid signatures of age-dependent early responses and of clinical adverse events

Olga Sobolev, Elisa Binda, Sean O'Farrell, Anna Lorenc, Joel Pradines, Yongqing Huang, Jay Duffner, Reiner Schulz, John Cason, Maria Zambon, Michael H Malim, Mark Peakman, Andrew Cope, Ishan Capila, Ganesh V Kaundinya & Adrian C Hayday
Nat. Immunol.; doi:10.1038/ni.3328; corrected online 7 January 2016

In the version of this article initially published online, the location of Momenta Pharmaceuticals was incorrectly stated as Boston. It should read "Cambridge." Also, in Table 1, the set of parentheses for HAI day 63 was incomplete. It should read "mean (s.d.)." The errors have been corrected for the print, PDF and HTML versions of this article.

Corrigendum: Adjuvanted influenza-H1N1 vaccination reveals lymphoid signatures of age-dependent early responses and of clinical adverse events

Olga Sobolev, Elisa Binda, Sean O'Farrell, Anna Lorenc, Joel Pradines, Yongqing Huang, Jay Duffner, Reiner Schulz, John Cason, Maria Zambon, Michael H Malim, Mark Peakman, Andrew Cope, Ishan Capila, Ganesh V Kaundinya & Adrian C Hayday

In the version of this article initially published, the affiliation for author Maria Zambon (Health Protection Agency, Porton Down, Salisbury, UK) was incorrect. The correct affiliation should be 'Public Health England, Colindale, London, UK'. The error has been corrected in the HTML and PDF versions of the article.